

# OPTIMIZATION OF TENSILE STRENGTH OF FERRITIC / AUSTENITIC LASER WELDED COMPONENTS

E. M. Anawa<sup>1</sup> and A. G. Olabi<sup>2</sup>

School of Mechanical & Manufacturing Eng., Dublin City University, Dublin 9, Ireland

1. [ezzeddin.hassan2@mail.dcu.ie](mailto:ezzeddin.hassan2@mail.dcu.ie), 2. [abdul.olabi@dcu.ie](mailto:abdul.olabi@dcu.ie)

## Abstract

Ferritic/Austenitic (F/A) joints are a popular dissimilar metals combination used in many applications. F/A joints are usually produced using conventional processes. Laser beam welding (LBW) has recently been successfully used for the production of F/A joints with suitable mechanical properties. In this study, a statistical design of experiment (DOE) was used to optimise selected laser beam welding parameters (laser power, welding speed, and focus length). The Taguchi approach was used for the selected factors, each having five levels (L-25; 5\*3). Joint strength was determined using the notched tension strength (NTS) method. The results were analysed using analyses of variance (ANOVA) and the signal-to-noise ratios (S/N) ratio for the optimal parameters, and then compared with the base material. The experimental results indicate that the F/A laser welded joints are improved effectively by optimizing the input parameters using the Taguchi approach.

**Keywords:** Ferritic Austenitic F/A, CO<sub>2</sub> laser beam welding, Notched-tensile strength, Taguchi approach.

## 1. Introduction

Laser welding is extremely advantageous in automotive applications due to its high power density, high degree of automation and a high production rate [1]. Joining low carbon steel (white ferrite), with 316 stainless steel (black austenite) is known as black and white joints. These dissimilar joints are based on both technical and economical aspects, because they can provide satisfactory service performance and reasonable cost savings. The demand for such joints in industry is huge; for example there can be over ten thousand such joints in a single power plant. [2]. Joining F/A is faced with the coarse grains phenomena in the weld and heat affected zone leading to low toughness and ductility due to the absence of phase transformation [3]. Joining F/A is considered to be a major problem due to the difference in thermal conductivities and thermal expansion, which may lead to crack formation (at the interface) or weld distortion [4,5,6]. Recently; laser beam applications in welding has received more attention for joining F/A. Mai, and Spowage, [7] carried out an investigation into laser welding of dissimilar metals without filler materials using Nd:YAG laser. They have studied the mixing behavior of the materials in the fusion zone, the microstructure, the presence of defects, hardness and residual stress of the joints. Zhang Li and G. Fontana [8] have investigated the feasibility of laser welding for joining AISI304L / AISI12L13. They have developed a technique (off-set and the impingement angle of the laser beam) for controlling solidification cracking and micro-fissuring.

Design of Experiment (DOE) and statistical techniques are widely used to optimize process parameters. Many investigations have been conducted to identify the optimal

process input parameters. Anawa and Olabi, [9] have used Taguchi parameter ‘design robust design’, as an optimization approach that uses a series of experiments (computer-based or physical) to find parameter settings for the design that yield predicted performance to be on target and as insensitive to noise as possible. Y. S. Tarng et. [10], have used a grey-based Taguchi method for the optimization of the submerged arc welding (SAW) process parameters in hard-facing with considerations of multiple weld qualities. They have used the grey relational grade obtained from the grey relational analysis as the performance characteristic in the Taguchi method. Then, optimal process parameters were determined by using the parameter design proposed by the Taguchi method. L. K. Pan et. al, [11] study was to optimize the use of an Nd:YAG laser for thin plate magnesium alloy butt welding using the Taguchi analytical methodology. In their study the welding parameters governing the laser beam were evaluated by measuring of the ultimate tension stress. This method was applied to reduce the number of experiments without affecting the results. The optimization of process parameters can improve quality characteristics; the optimal combination of the process parameters can then be predicted. This work was concerned with the effects of welding parameters on the tensile strength of F/A joints and the prediction of the optimal combinations of the welding parameters. The objective of this study is to optimize the maximum ultimate tensile strength of F/A welded components, by minimizing the laser power and maximizing welding speed in order to optimize the cost and increase the production rate.

## **2. Experimental Design**

Experiments were designed by the Taguchi method using an L-25 orthogonal array that was composed of 3 columns and 25 rows. This design was selected based on three

welding parameters with five levels each. The selected welding parameters for this study were: welding power, welding speed and focus point position. Pilot experiments of laser welding were carried out to determine the practical operating range of each individual selected laser welding parameters in order to produce an acceptable quality welding of the dissimilar materials. Assessment welding trials were made by fixing the welding parameters and changing one at a time for each dissimilar joint materials. Visual inspections for the joints were applied to decide the parameter operating range. The visual inspections were applied for detection of welding defects: Surface flaws - cracks, porosity, unfilled craters, slag inclusions, poorly formed beads, misalignments and/or un-full penetration in some cases, and at the same time to check the status of the fine welding seam. The obtained welding seam of selected specimen is exhibited in Fig. 1. Table 1 show the practical operating range the laser input variables and experiment design levels. The Taguchi method was applied to the experimental data using statistical software, "Design-expert 7". Usually, there are three categories of quality characteristic in the analysis of the S/N ratio, i.e. the smaller-the-better, the bigger-the- better and the nominal-the-better. The S/N ratio for each level for each of the process parameters is computed based on the S/N analysis. Regardless of the category of the quality characteristic, a larger S/N ratio corresponds to a better quality characteristic. Therefore, the optimal level of the process parameters is the level with the highest S/N ratio. A statistical analysis of variance (ANOVA) was also performed to indicate which process parameters are statistically significant; the optimal combination of the process parameters can then be reproduced. Finally, confirmation experiments were conducted to verify the optimal process parameters obtained from the design.

### 3. Experimental Work

In this work, two plates of mild carbon steel and AISI 316 stainless steel with maximum tensile strength of 350 MPa and 600 MPa respectively were used; the chemical compositions of these materials are presented in Table 2. The dimension of each plate is 160 x 80 x 2 mm. A butt joint was applied for joining the two plates together. In the course of this work, the plate's edges were cleaned and grinded along the weld line to ensure full contact. No special heat treatments were carried out before or after laser welding. The experiments were carried out according to the design matrix given in Table 3. They were performed in random order to avoid any systematic error. A CW 1.5 kW CO<sub>2</sub> Rofin laser with 127 mm focal length high pressure lenses and 10.6 μm wavelength, provided by Mechtronic Industries Ltd, was used. Argon gas was used as a shielding gas with a constant flow rate of 5 ℓ/min. Notched tensile strength (NTS) samples exhibited in Fig. 2 were produced from the jointed samples by laser cutting within the same laser machine used for welding. The notched tensile strength test was applied to ensure that the fracture of the sample will occur in the welding area, because the tensile strength of the produced joints is higher than the tensile strength of both base metals. NTS samples were tested at room temperature of 20 °C and the pooling direction was perpendicular to the welding line. Instron Universal Electromechanical testing machine used, model 4202, with a gauge length of 25 mm and crosshead speed of 0.75 mm min<sup>-1</sup>, the correspondence strain rates was 5 x 10<sup>-4</sup> s<sup>-1</sup>. The average of at least three results of NTS was calculated for each sample. Table 3 illustrates the experimentally measured responses.

## 4. Results and Discussion

### 4.1. Orthogonal array experiment and the signal-to-noise (S/N) ratio

In this study, an (L-25; 5\*3) orthogonal array with three columns and 25 rows was used. This array can handle five-level process parameters. Twenty-five experiments were required to study the welding parameters using L25 orthogonal array. In order to evaluate the influence of each selected factor on the responses: The signal-to-noise ratios S/N for each control factor had to be calculated. The signals have indicated that the effect on the average responses and the noises were measured by the influence on the deviations from the average responses, which would indicate the sensitiveness of the experiment output to the noise factors.

The suitable S/N ratio must be chosen using previous knowledge, expertise, and understanding of the process. When the target is fixed and there is a trivial or absent signal factor (static design), it is possible to choose the S/N ratio depending on the goal of the design. In this study, the S/N ratio was chosen according to the criterion the-bigger-the-better, in order to maximize the responses.

The S/N ratio for “bigger is better” target for all the responses were calculated as follows:

$$S/N = -10 \log_{10} \left[ \sum \frac{1/y^2}{n} \right]$$

Where: y is the average measured tensile strength, n the number of experiment runs, in this study = 25.

The experimental layout for the welding process parameters using the L25 orthogonal array is shown in Table 3 and the responses for signal-to-noise ratio S/N are presented in Table 4. The main effects plots exhibited in Fig. 3 show that how each factor affects the response characteristic. This can present the different levels of a factor affect the characteristic differently. The main effects plot created by MINITAB is plotting the characteristic average for each factor level. These averages are the same as those displayed in the response table. The average NTS tests appear to be mainly affected by the laser power and welding speed as shown in Table 4. The rank 1 in Table 4 indicates that power parameter (1) has stronger effect on the process followed by rank (2) speed which has less effect, while rank (3) has the minimum or no effect on the process.

#### **4.2. ANOVA**

The purpose of the ANOVA is to investigate which welding process parameters significantly affect the quality characteristic. This is accomplished by separating the total variability of the S/N ratios, which is measured by the sum of the squared deviations from the total mean of the S/N ratio, into contributions by each welding process parameter and the error [10]. To analyze the effects of the welding parameters in detail, backward regression method; which eliminates the insignificant model terms automatically was applied for the developed model and the results are exhibited in ANOVA Table 5.

In the ANOVA table, Table 5, the F Value is used to test the significance of a factor by comparing model variance with residual (error) variance, which is calculated

by dividing the model mean square by the residual mean square. If the variances values are close to each other, the ratio will be close to one and it is less likely that any of the factors have a significant effect on the response. A high F value for a parameter means that the effect of the parameter on the characteristics is large. The result in Table 5 shows that the highest F value in the process was obtained for laser power (P) equal to 25.35. The F value for the speed (S) was equal to 3.85, which indicates that the speed has a relatively less effect on the process. Adequate Precision compares the range of the predicted values at the design points to the average prediction error. Ratios greater than 4 indicate adequate model discrimination. For this model it was equal to 11.580, as shown in Table 5. The same table also shows the other adequacy measures  $R^2$  and Adjusted  $R^2$ . All the adequacy measures indicate that an adequate model has been obtained. The final mathematical model for predicting the tensile strength of dissimilar F/A joint in terms of actual factors as developed by Design Expert software is shown below.

$$\textit{Tensile Strength} = 428.917 + 223.514 * P - 0.065 * S$$

### 4.3. Validation of the Model

Fig. 4 shows the actual response versus the predicted response for NTS. From this figure, it can be seen that the model adequately describes the response within the limits of the factors being investigated herein, as the data points are close to the diagonal line. Furthermore, three extra confirmation experiments were carried out using the developed model with different parameters conditions, which are presented in Table 6 along with the resulting percentage error. It can be noticed that the NTS value obtained after laser



welding is greater than the base metals value specially when compared to low carbon steel side.

#### **4.4. Effect of Process Parameters on the Response:**

1) **Laser power:** It can be seen that the laser power is the most significant factor associated with the response, as shown in Fig. 3. It is clear that the higher laser power resulted in a higher response value, due to the fact that using high laser power would increase the power density. This leads to more penetration resulting in an improved response [9]. The relationship between the welding parameters (P, S at F = -.92mm) and the tensile strength of the dissimilar jointed components is exhibited by contour graph in Fig. 5.

2) **Welding speed:** It is evidence from the results that the welding speed also has a strong effect on the tensile strength of the laser-welded joint, as shown in Fig. 3. The highest tensile strength value was observed to be at a speed of 500 mm/min. It is evidence that by increasing welding speed with or without changing focus position the response would decrease.

3) **Focus point position:** The results indicate that the focus point position has no obvious effect on the response within the parameter range domain applied. By changing the focus point position the response will not be effected.

## **5. Micro harness and microstructure studies**

### **5.1. Microstructure in the HAZ**

Refers to the epitaxial nature of solidification, the grain boundary in the HAZ can link up with the solidification grain boundary in the fusion zone. Segregation of S, Pb, Mn and P during solidification means that these elements are able to diffuse into the HAZ from the fusion zone along the grain boundaries. The dissolved elements and impurities diffuse more rapidly along the grain boundaries than through the crystal lattice, and this result in a local reduction of the melting temperature.

The microstructures in the fusion zone are a result of solidification behavior and subsequent solid-phase transformation, which are controlled by composition and weld cooling rates. Moreover, the composition in the fusion zone of a dissimilar joint depends on the melting ratio of the two materials to be jointed, which in turn is related to the welding parameters. Figs. 6 (a, b), shows the redistribution of elements in the fusion zone of a butt weld joining AISI316 to AISI1008, corresponding to the welding parameters given in Table 3 of the specimens number 1 and 25 respectively . It is obvious from Figs. 6 (a, b) the HAZ of AISI1008 width is about 300 to 400  $\mu\text{m}$  while the HAZ of AISI316 width is about 60 to 70  $\mu\text{m}$ , this is due to that the thermal expansion coefficient of austenite being higher than that of ferrite, and the heat conductivity of austenite is lower than that of ferrite, these features resulted in a higher level of thermally-generated stresses.

## 5.2. Microhardness

Since AISI316 is an austenitic base material and AISI1008 is a ferritic base material, the microstructures of the fusion zone must contain a variety of complex austenite–ferrite structures. Fig. 7 shows the microhardness profile of the joint in seven different points of selected specimens. The specimens selected for microhardness studies were based on heat input calculations ( $P \times S$ ). The microhardness of the fusion zone is greater than that of both the AISI316 and AISI1008 base materials; this may result from the effect of rapid solidification. The microhardness gradient correlates with the gradient of the redistribution of the elements Cr, Fe, and Ni, which may be a particular phenomenon of dissimilar fusion joints. The cooling rate in the fusion zone of laser keyhole welds is roughly between  $10^4$  and  $10^6$  °C  $s^{-1}$ . Rapid solidification not only increases under cooling and nucleation probability, which leads to very fine structures but also extends the solutes solubility, which thus prevents marked segregation and results in a supersaturated solid solution, and then new microstructures and this result is in close agreement with L. Nastac and D.M. Stefanescu [12]. The microhardness of the weld HAZ interface in both sides is less than that measured in the weld pool but it is higher than the HAZ and base metals. This is due to the rapidly solidification as mentioned above.

The strength of the laser welds is higher than the tensile strength of AISI316 / AISI1008 under the test conditions adopted in this study. The greater tensile strength of the laser welds demonstrates the beneficial effect of rapid solidification in the fusion

zone and of a small HAZ. The microstructures in the fusion zone call for further research using TEM.

## **6. Conclusion**

F/A joints are a popular dissimilar metal combination used in many applications. Therefore, exploitation of new processes for producing these joints is of interest to several industrial sectors. The following points can be concluded from this study:

- i) Laser welding is very successful process to join stainless steel and low carbon steel.
- ii) Laser power is the main factor affecting the response. The speed also has a strong effect on the response; increasing welding speed will lead to a decrease in response. But focus position had no obvious effect on the tensile strength of the produced welded components.
- iii) The F/A welding joints produced have better mechanical properties compared to the base metals due to the beneficial effect of rapid solidification in the fusion zone and of a small HAZ resulted by laser welding.
- iv) The model developed can adequately predict the response within the factors domain. The optimum tensile strength value reached by the new developed model and using the Design Expert software; was 656 MPa which was obtained at a speed of 1000mm/min, laser power of 1.31 kW and focus position of -0.67 mm.

## **Acknowledgement**

The Libyan educational ministry is gratefully acknowledged for the financial support of this research. Technical support from Mr. Martin Johnson and Mr. Michael May and Dublin City University are also gratefully acknowledged.

### **List of Figures**

Fig. 1, Shows the laser welding process of two plates of mild low carbon steel and AISI 316 stainless steel

Fig. 2, the notched tensile strength (NTS) specimen

Fig. 3, Effect of the laser welding parameters on the tensile strength and S/N ratio

Fig. 4, Predicted Vs Actual for notched tensile strength NTS, M Pa

Fig. 5, contour graph shows the relationship between welding parameters (P, S) and the tensile strength of the dissimilar components at  $F = -0.92$ .

Figs. 6 (a, b) shows the redistribution of elements in the fusion zone of a butt weld joining AISI316 to AISI1008

Fig. 7, the microhardness profile of the dissimilar joint for the specimens (1, 5, 7, 15, 22 and 25)



**Fig. 1,** Shows the welding seams of laser welding of low carbon steel jointed to AISI 316 stainless steel.

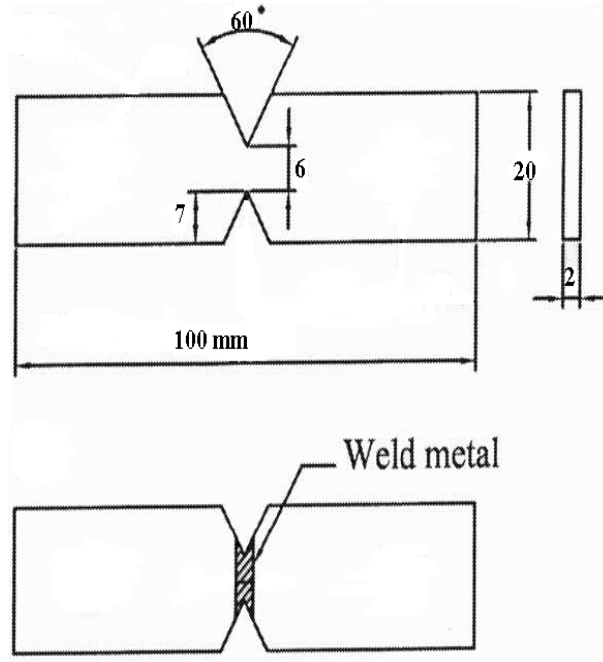


**Fig. 2,** The notched tensile strength (NTS) specimen

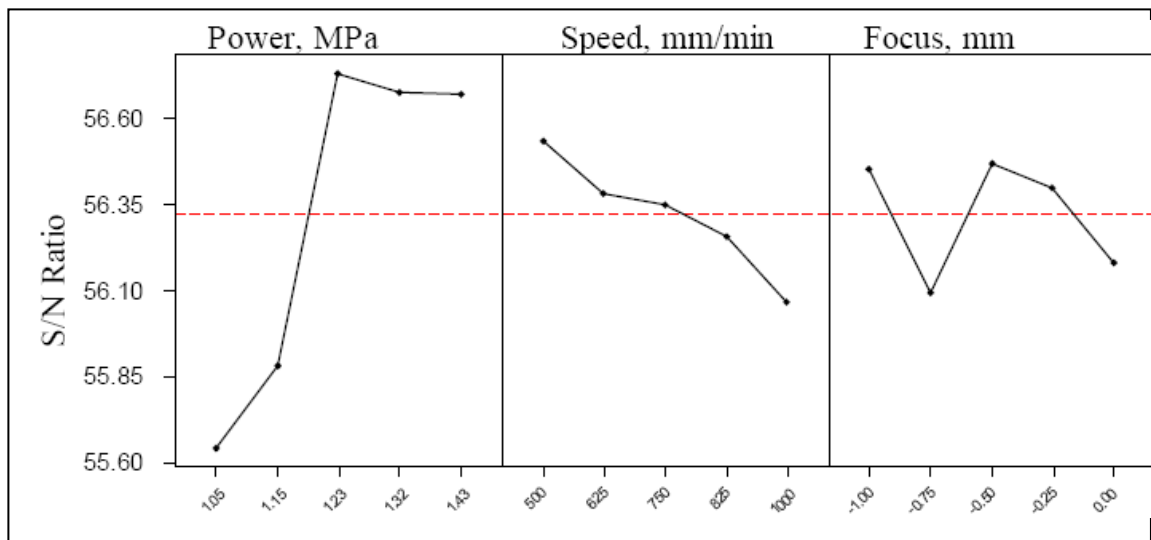


**Fig. 3,** Main effects plot for S/N ratios



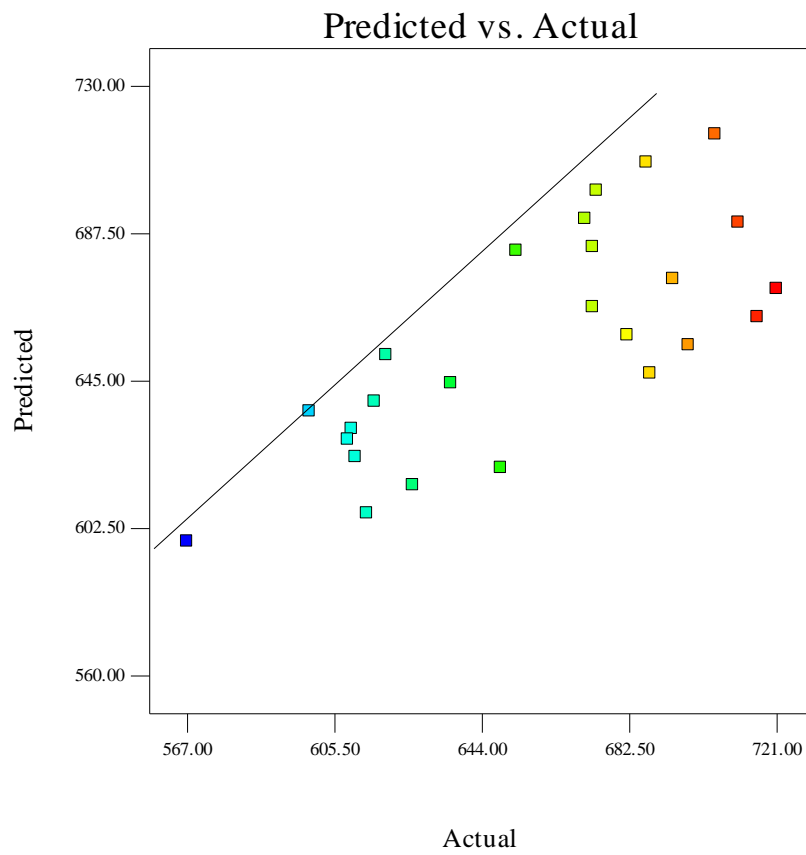


**Fig. 4,** Predicted Vs Actual for notched tensile strength NTS, M Pa.

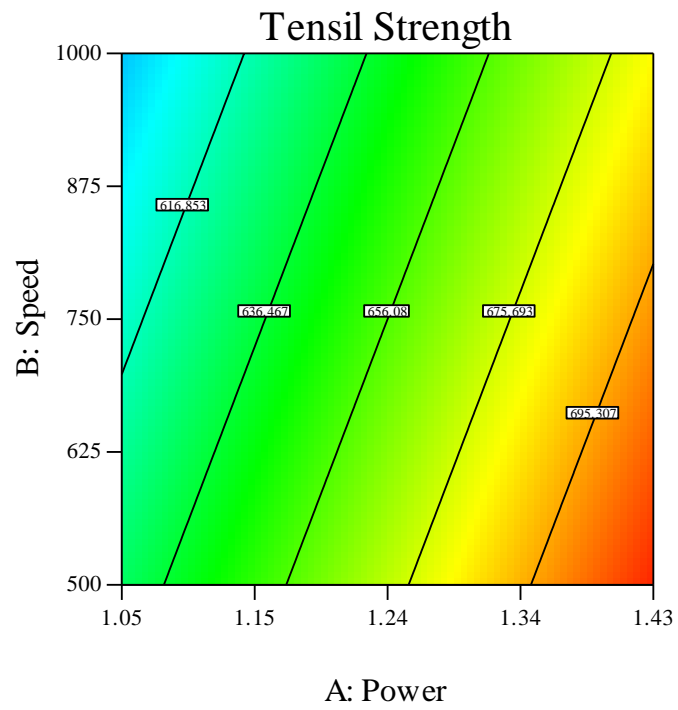


**Fig. 5**, contour graph shows the relationship between welding parameters (P, S) and the tensile strength of the dissimilar components at  $F = -0.92$ .

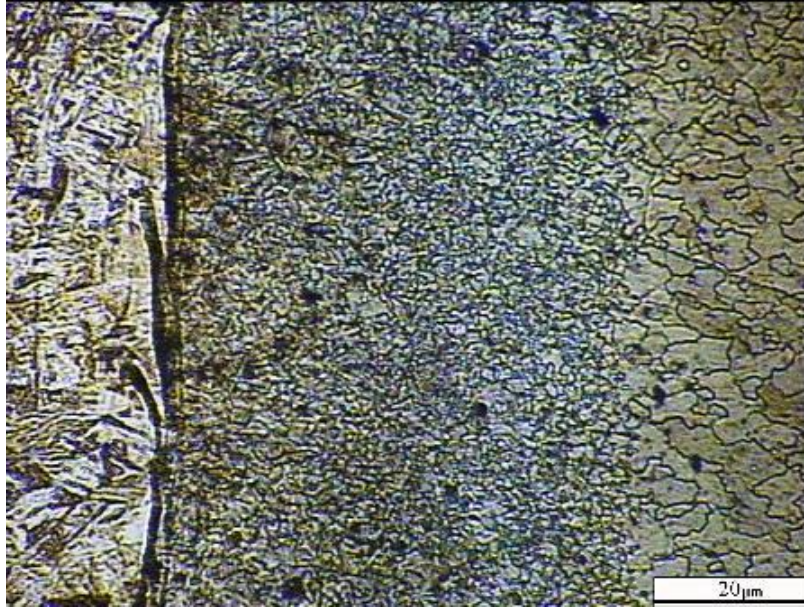


**Fig 6(a),** Weld pool, HAZ and BM of AISI1008.

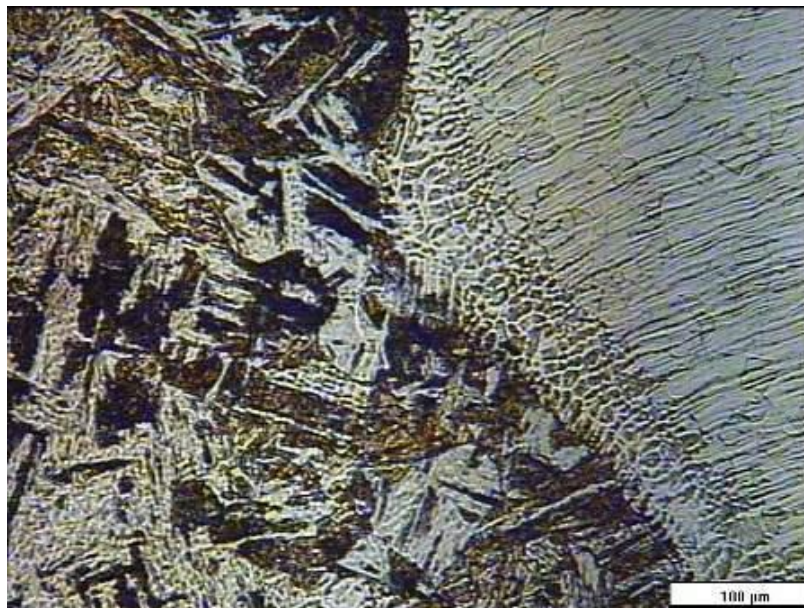


**Fig 6(b)**, Weld pool, HAZ and BM of AISI316.

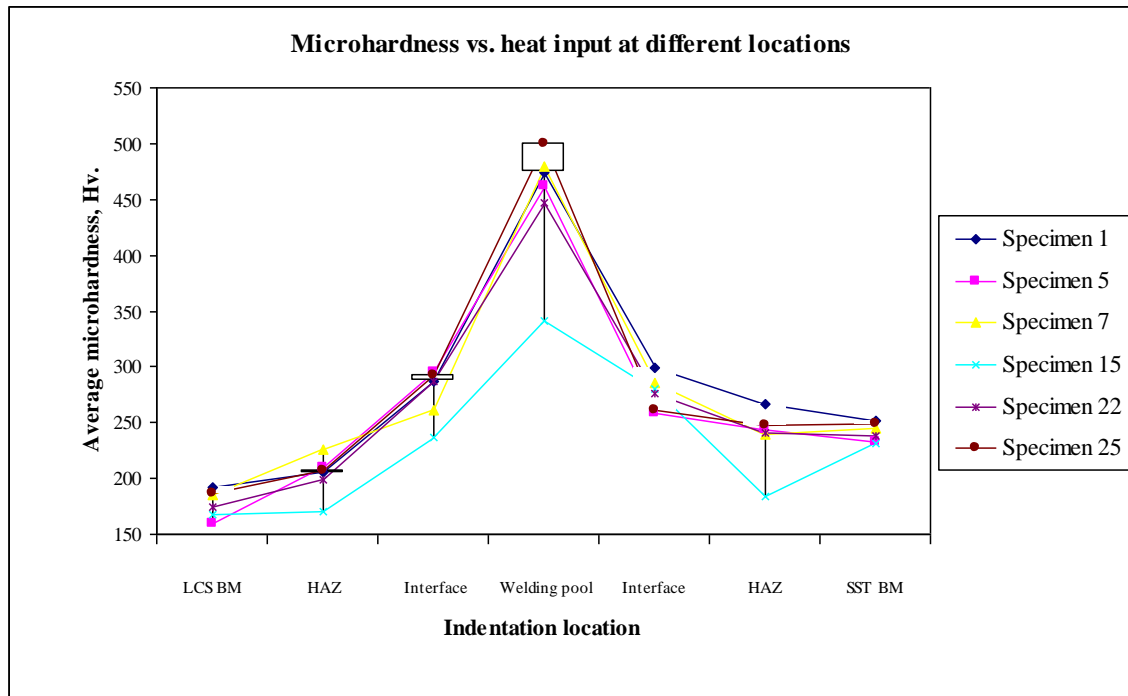


**Fig. 7**, The microhardness profile of the dissimilar joint for the specimens (1, 5, 7, 15, 22 and 25).

**List of Tables**

Table 1, Process parameters and design levels used.

Table 2, Chemical composition of the jointed materials (wt %)

Table 3, Experimental assignments, response, and S/N ratio

Table 4, Response for S/ N Ratio

Table 5, ANOVA for selected factorial model.

Table 6, Confirmation experiments of the responses compared with model results.

**Table 1, Process parameters and design levels used**

Variables	Code	Unit	Levels				
			1	2	3	4	5

Laser Power	P	kW	1.05	1.15	1.24	1.33	1.43
Welding Speed	S	mm/min	500	625	750	825	1000
Focused position	F	mm	-1	-0.75	-0.5	-0.25	0

**Table 2,** Chemical composition of the materials (wt %)

Material	C	Si	Mn	P	S	Cr	Ni	Nd	Mo	Fe
LCST*	0.093	0.027	0.210	0.001	0.005	0.043	0.065	0.024	0.006	Bal.
316SST	0.048	0.219	1.04	0.013	0.033	18.028	10.157	0.098	1.830	Bal.

LCST\* - AISI1008 low carbon steel.

**Table 3, Experimental assignments, response, and S/N ratio**

Exp. No.	Input Parameters			output s		Exp · No.	Input Parameters			outputs	
	P kW	S mm/min	F mm	NTS MPa	S/N		P kW	S mm/ min	F mm	NT S MP	S/N

										<b>a</b>	
1	1.05	500	-1.00	610	55.71	14	1.23	875	-1	688	56.75
2	1.05	625	-0.75	611	55.72	15	1.23	1000	-0.75	616	55.79
3	1.05	750	-0.50	626	55.93	16	1.33	500	-0.25	711	57.04
4	1.05	875	-0.25	614	55.76	17	1.33	625	0	653	56.30
5	1.05	1000	0.00	567	55.07	18	1.33	750	-1	694	56.83
6	1.15	500	-0.75	619	57.13	19	1.33	875	-0.75	673	56.56
7	1.15	625	-0.50	636	56.07	20	1.33	1000	-0.5	682	56.68
8	1.15	750	-0.25	599	55.55	21	1.43	500	0	705	56.96
9	1.15	875	0.00	609	55.69	22	1.43	625	-1	687	56.74
10	1.15	1000	-1.00	649	56.24	23	1.43	750	-0.75	674	56.57
11	1.23	500	-0.50	721	57.16	24	1.43	875	-0.5	671	55.75
12	1.23	625	-0.25	716	57.10	25	1.43	1000	-0.25	673	56.56
13	1.23	750	0.00	698	56.88	-	-	-	-	-	-



**Table 4,** Response for S/ N Ratio

Levels	1	2	3	4	5	Delta	Rank
P	55.64	55.88	56.74	56.68	56.67	1.10	1
S	56.54	56.38	56.35	56.26	56.07	0.47	2
F	56.45	56.09	56.47	56.40	56.18	0.38	3

**Table 5,** ANOVA for selected factorial model

Source	Sum of Squares	df	Mean Square	F Value	p-value Prob. > F	
Model	25011	2	12505	14.60	< 0.0001	<b>significant</b>
P	21714	1	21714	25.35	< 0.0001	

S	3297	1	3297	3.85	0.0626	
Residual	18847	22	857			
Cor Total	43858	24				
$R^2 = 0.5703$				Adeq. Precision = 11.580		
$Adj. R^2 = 0.5312$						

**Table 6,** Confirmation experiments of the responses compared with model results

<b>Exp. No</b>	<b>P, kW</b>	<b>S, mm/min</b>	<b>F, mm</b>	<b>Tensile strength, MPa</b>		$ E\% $
				<b>Actual</b>	<b>predicted</b>	
1	1.05	500	-0.75	589	631	7.1
2	1.20	750	0	658	648	1.5
3	1.28	1000	-0.29	603	650	7.7

## References

- 
- [1] C. Dawes, Laser welding, Abington Publishing, New York, 1992.
- [2] Z. Sun, Feasibility of producing ferritic/austenitic dissimilar metal joints by high energy density laser beam process, Int. Journal of pres. And Piping vol.68 (1996) 153-160.
- [3] V .V Satyanarayana, T. Mohandes, Dissimilar metal friction welding of austenitic–ferritic stainless steels, Journal of Materials Processing Technology, 160 (2005) 128-137.

- 
- [4] S. Allabhakshi, G. Madhusudhan Reddy, V.V. Ramarao, C. Phani Babu, C.S. Ramachandran, Studies on weld overlaying of austenitic stainless steel (AISI 304) with ferritic stainless steel (AISI 430), National Welding Conference, Chennai, India, January 2002, Indian Institute of Welding, Paper 8.
- [5] A. Omar, Effects of welding parameters on hard zone formation at dissimilar metal welds, *Weld. Journal*. 77 (2) (1998) 86s–93s.
- [6] *Welding HandBook*, 7th ed., vol. 4, American Welding Society, 1984, pp. 93–128.
- [7] T. A. Mai, A. C. Spowage, Characterisation of dissimilar joints in laser welding of steel–kovar, copper–steel and copper–aluminium, *Journal of Material Science and Engineering A* 374 (2004) 224-233.
- [8] Z. Li, ,Autogenous laser welding of stainless steel to free-cutting steel for the manufacture of hydraulic valves, *Journal of Materials Processing Technology* 74 (1994) 174-182.
- [9] E.M. Anawa and A.G. Olabi, Using Taguchi method to optimize welding pool of dissimilar laser-welded components, *Optics & Laser Technology*, Volume 40, Issue 2, March 2008, Pages 379-388
- [10] Y. S. Tarng and S. C. Juang, The use of grey-based Taguchi methods to determine submerged arc welding process parameters in hard facing, *Journal of Materials Processing Technology*, Volume 128, Issues 1-3, 6 October 2002, Pages 1-6.
- [11] L. K. Pan, Che Chung Wang, Ying Ching Hsiao and Kye Chyn Ho, Optimization of Nd:YAG laser welding onto magnesium alloy via Taguchi analysis, *Optics & Laser Technology*, Volume 37, Issue 1, February 2005, Pages 33-42.

---

[12]L. Nastac, D.M. Stefanescu, An analytical model for solute redistribution during solidification of planar, columnar, or equiaxed morphology, *Met. Trans. A* 24A 1993, pp. 2107–2118.